Soft-landed ion diffusion studies on vapor-deposited hydrocarbon films

A. A. Tsekouras
Laboratory of Physical Chemistry, University of Athens, Athens, GR-15771, Greece

M. J. Iedema and J. P. Cowin[a)]
Pacific Northwest National Laboratory, Box 999, M/S K8-88, Richland, Washington 99352

(Received 22 January 1998; accepted 22 April 1999)

Cesium and hydronium ions were deposited with a ''soft-landing'' ion beam (1 eV) on *n*-hexane and 3-methyl-pentane vapor-deposited thin films on a Pt (111) surface at 27 K. Dielectric properties and ion migration were studied during the ion deposition and during a temperature ramp up to the desorption temperature of the molecular films. The ions were found to migrate through amorphous versions of these films as expected by simple viscosity models near 90 K with ion mobilities of about $10^{-18}\,m^2\,V^{-1}\,s^{-1}$. No, or very limited, diffusion was observed through crystalline films. The *n*-hexane films crystallize during the ion motion. Analysis of this permits the estimation that average diffusional motion for a neutral hexane during crystallization is about 1 molecular diameter. © *1999 American Institute of Physics.* [S0021-9606(99)72127-6]

I. INTRODUCTION

Transport properties of ions through organic layers are central to topics as diverse as cell wall transport, fuel cells, chemical sensor electrodes, reactions and separations using nonaqueous solvents, organic electronics, photographic film, and food packaging. It is often difficult to measure ion mobility in organic materials, as it has usually not been possible to create systems where the ion identity, transport distance, and times are all simultaneously well defined. This is especially true in most organic solvents, as the concentrations of such ions are severely limited by the very sparing solubility of most ionic species in these nonaqueous solvents.

Using our newly developed soft-landing ion source,[1] we can overcome these difficulties in a most direct way. We fabricate amorphous (or crystalline) films with monolayer precision by molecular beam deposition, and gently place on or within them pure, mass-selected, chemically relevant ionic species from our 1 eV ion beam. Amorphous films above their glass transition temperatures are true liquids, but have advantages of low vapor pressure, compatible with vacuum instrumentation, and slow enough kinetics (seconds to hours) to allow careful setup of geometries, and detailed measurements of the rates to be made.[2] These experiments are in many ways a realization of a ''thought experiment'' on recreating electrochemical double layers in ultrahigh vacuum discussed by Wagner in Ref. 3. Soft-landed ions are a powerful new tool, now being exploited by a handful of researchers[4] to probe a variety of interfacial problems.

In this experiment, we measured work function changes created when ions were soft landed on a thin film under study. We will show how ion motion through 3-methyl pentane is very simple and matches expectations given the known viscosity of the material. Through *n*-hexane, we show that the mobility permitting ion motion also permits crystallization. However, before crystallization, the ions move with a field-proportional drift velocity, up to the mid 10^8 V/m range.

Before proceeding with the experimental results, we present simple capacitor and ion mobility relations.

An organic layer like hexane ice deposited on a metal surface would be expected to act like an insulating, linear dielectric medium, at least for not too intense electric fields. Ions of charge nq_e placed on top of it should create a voltage due to their charge and the capacitance of the ice film. This voltage creates a change in the work function ϕ of the metal+film assembly by an amount

$$\Delta\phi = -Q/C, \tag{1}$$

where the capacitance C is given by

$$C = \frac{A\varepsilon\varepsilon_0}{L}. \tag{2}$$

Thus,

$$\Delta\phi = \frac{-QL}{A\varepsilon\varepsilon_0} \equiv -\Delta V_{\text{film}}, \tag{3}$$

where Q is the charge deposited, A the area, L the film thickness, ε the film permittivity (dielectric constant), ε_0 the vacuum permittivity, and ΔV_{film} we define as the ''film voltage.''

When ε is constant, as it nearly is for hexanes, the motion of the ions can be tracked by changes in the work function. Motion of the ions into the film will create within the ice film a charge distribution of ions given by $\rho(x,y,z)$. Generally, we expect the x and y dependence of the ion density to be small. But more importantly, the macroscopic film voltage is only sensitive to the density averaged over x and y, to give $\rho(z)$. Integration (by parts) of the Poisson equation over the free charges, in the presence of a *constant* dielectric material, can be shown to yield the simple expression for the voltage across the film (in the absence of significant externally applied fields)

a)Electronic mail: jp_cowin@pnl.gov

$$V(L)-V(0)=\Delta V_{\text{film}}=\int_0^L dz\,\frac{\rho(z)z}{\varepsilon\varepsilon_0}=\frac{Q\langle z\rangle}{A\varepsilon\varepsilon_0}=-\Delta\phi, \qquad (4)$$

where $\langle z\rangle$ is the average ion height within the ice film. By comparing with Eq. (3), we see that $\langle z\rangle$ replaces L when the ions move. This means that if we follow the changes in the work function induced by the ions as the temperature is increased, we are essentially measuring the evolution of the average ion height within the film. This is again supposing that the ice has a linear and constant dielectric constant during the temperature changes (a fairly good assumption for nonpolar hexanes), no changes in film density are occurring (not necessarily justified, especially for amorphous films[5,6]), and no discharging of the ions occurs via electron transfer (this would change both $\langle z\rangle$ and Q).

Ions, once on or within the film, can move by two classic means; random, thermally assisted migration, and the systematic drift motions that occur under the influence of an external electric field E.[7] The random motion involves the diffusion coefficient D, whereas the drift velocity v is proportional to the applied electric field (at not too high a field strength) with the ion mobility μ as the proportionality factor. The Einstein relation [Eq. (5)] links D and μ, and the result for the evolution of the number distribution $\rho(z)$ of positive ions of charge nq_e is Eq. (6)

$$D=\frac{\mu(T)kT}{nq_e}, \qquad (5)$$

$$\frac{d\rho(z)}{dt}=D\,\frac{d^2\rho(z)}{dz^2}-\mu(T)\,\frac{d(\rho(z)\mathbf{E}_z(z))}{dz}, \qquad (6)$$

$$\frac{\text{random diffusion time}}{\text{field-assisted drift time}}\approx\{L^2/D\}\Big/\left\{\frac{L}{\mu q_e n^{\Delta V_{\text{film}}/L}}\right\}$$

$$=\frac{\Delta V_{\text{film}}q_e n}{kT}. \qquad (7)$$

The last expression is the ratio of the times to traverse the film via random diffusion and field-assisted drift. For a 10 V film voltage at 150 K, the ion mobility is around 1000 times more effective than the random migration, and thus we can neglect the first term in Eq. (5).

II. EXPERIMENT

The experiments were performed in an ultrahigh vacuum apparatus[1] designed for surface science studies (see Fig. 1). A base pressure of 2×10^{-10} torr was maintained with a 400 l/s ion pump (Thermionics).

A crystal manipulator, attached to a fully rotatable lid, supported a vertically mounted Pt(111) crystal (1 cm diameter), allowing positioning through rotation around a vertical crystal diameter and translation. A helium closed-cycle refrigerator could reduce the temperature to 27 K and a set of four tungsten filaments on the back side of the crystal was used to radiatively heat it to 1300 K using a feedback system. Two nickel–chromium/nickel–aluminum (type K) thermocouples, spot welded to the edges of the crystal, monitored the temperature and provided the electrical connection

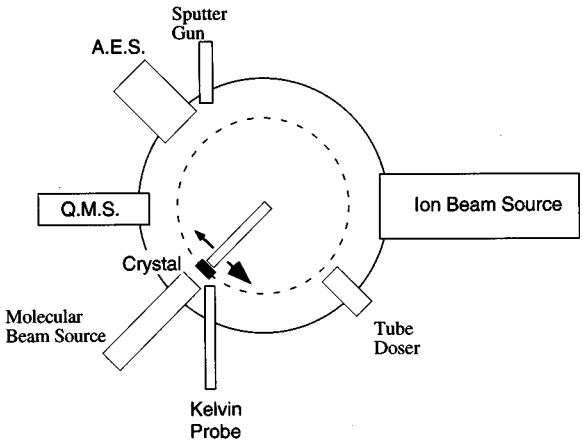

FIG. 1. Experimental apparatus. Top view of the main components of the UHV chamber (arranged on two different vertical levels).

to the crystal for biasing it and measuring the ion current. The thermocouple voltage was measured by a digital voltmeter (Keithley 612) interfaced to the computer controlling the experiment. The thermocouple voltage was also monitored by a temperature controller (Eurotherm 900) that drove the filament crystal heater supply. Ion current to the crystal was measured with a floating electrometer (Keithley 614) connected to an appropriate bias source. Its output was sent via an isolator to the computer.

The crystal could be positioned in front of any of the following instruments located on the walls of the chamber. A molecular beam source was used to deposit known amounts of *n*-hexane or 3-methyl-pentane (3MP) vapor (from repetitively freeze–thaw-degassed liquids). It consists of a large 0.2 mm nozzle (run nearly effusive to suppress cluster formation that strong supersonic expansion could create), expanding into a chamber with a 100 l/s diffusion pump. The beam passes through two more short chambers, each pumped by a 60 l/s turbomolecular pump, before passing into the ultrahigh vacuum chamber. An undifferentially pumped aperture near the Pt(111) substrate removes the slight beam ''penumbra,'' to make the dosing quite uniform over the central 0.9 cm of the 1.0 cm of crystal, at normal incidence. The nozzle is about 44 cm from the Pt substrate. A typical beam flux on the crystal was 1 *n*-hexane monolayer per 8 s. An Auger spectrometer was used to inspect surface cleanliness. A sputter gun was used occasionally if persistent carbon, calcium or indium (from an earlier encounter with a drop of melted indium) was detected at or above a percent level. A computer-driven quadrupole mass spectrometer with electron impact ionization (Extrel) monitored the amounts of gases desorbing from the crystal.

The ion source[1] consisted of several differentially pumped stages with ion optics that ensured beam uniformity, low energy spread, low neutral load, and ion selectivity. Cs^+ ions were emitted from a porous tungsten dispenser (Heat-Wave, Inc.), accelerated to 300 eV to travel the majority of the length of the beam, finally to be decelerated just in front of the crystal in a short, planar decelerator consisting of a double mesh and the crystal. The final energy when reaching the crystal was near 1 eV. D_3O^+ ions were created by colli-

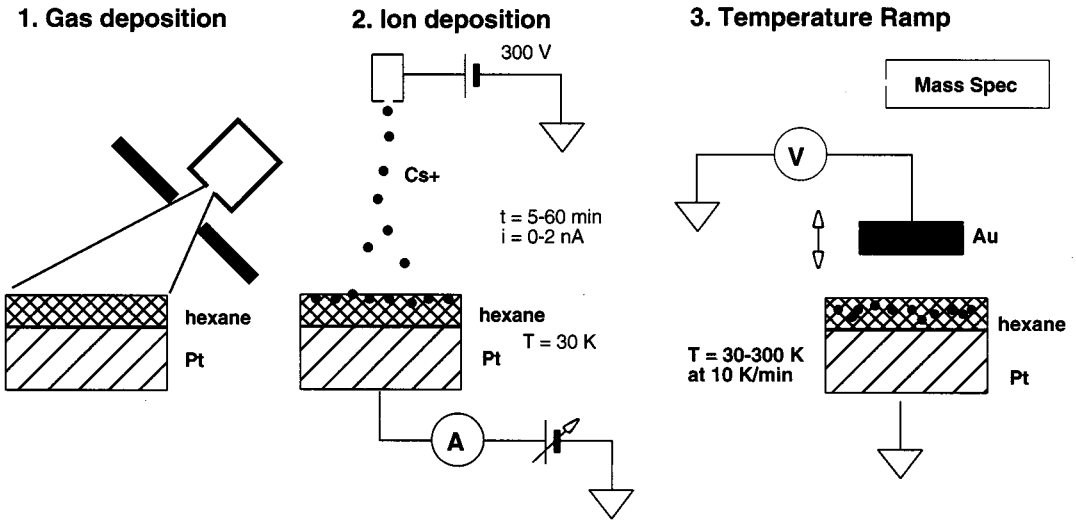

FIG. 2. Experimental procedure. (1) *n*-hexane deposited at 27–30 K as amorphous layer, occasionally annealed to form a crystalline layer. (2) Energy of deposited ions was controlled by the bias difference between the ion source and the crystal. (3) Temperature programmed desorption spectra and film voltages were recorded during the temperature ramp.

sions of 150 eV electrons in the expansion region of a pure D_2O beam, creating D_2O^+ that then collided with neutral water molecules in the expanding molecular beam to form D_3O^+ and DO. The D_3O^+ was separated from other ionic species present using a Colutron Wien filter, and delivered to the crystal the same way as with Cs^+ ions.

Charging of the crystal surface and work function changes were measured using an oscillating, gold-plated electrode (Kelvin Probe 6000, McAllister Technical Services) equipped with digital and analog output. A few millivolts precision was achieved through proper electrical grounding (enhanced by elimination of stray electrons emitted from the mass spectrometer), mechanical stability (achieved by temporary interruption of the He closed-cycle refrigerator and relying on a large copper block's heat capacity to maintain low temperatures), and maximizing rejection of 60 Hz noise by digitizing for integer multiples (8 and 14) of periods for both 60 Hz and the Kelvin probe frequency of 105 Hz.

A typical experiment was performed in three stages (see Fig. 2). First, a layer of adsorbate was deposited on the surface of a clean Pt (111) crystal. Then, an ion beam with energy below 1.2 eV and currents up to 2 nA was aimed at the crystal at normal incidence creating a layer of ions on top of the molecular adsorbate. During this deposition of ions, the film would charge like a capacitor. This charging, as is shown in detail later, could easily be monitored during the ion deposition. This changes the ion impact energy, decreasing it, and it was important to keep compensating for this during ion deposition by changing the crystal bias. The final measurement consisted of simultaneously monitoring adsorbate partial pressure in the gas phase and crystal work function during a sample temperature ramp, using the mass spectrometer and the Kelvin probe, respectively.[5] The total ions deposited tended to be on the order of 0.1% of the platinum surface atoms, and typically produced a negligible change in work function when deposited directly on the Pt substrate ($\langle z \rangle$ near zero), with or without an ice film above the ions.

III. RESULTS

A. Thermal desorption/adsorption

Temperature programmed desorption (TPD) spectra were recorded between 30 and 300 K at ramp rates as low as 0.05 K/s (for simultaneous Kelvin probe measurements) to 5 K/s. The first monolayer desorption for *n*-hexane with a heating rate of 5 K/s took place at 240 K, the second monolayer peak appeared at 149 K, and the multilayer peak appeared for low coverages near 144 K [see Fig. 3(a)] and higher for higher coverages. This is in good agreement with similar published adsorption studies of *n*-hexane.[8,9] The coverage that just saturates the high temperature peak gives the known surface density of *n*-hexane of $2.1\times10^{14}\,\mathrm{cm}^{-2}$ (or 48 Å^2/molecule).[10] The integral (versus time) of the first monolayer peak TPD also provided a calibration of the amount adsorbed for all coverages. A plot of the TPD integral versus molecular beam dosing time (see Fig. 4) consists of a nearly straight line passing nearly through the origin, indicating a constant sticking probability at coverages greater than one monolayer, probably equal to 1. The slope is less below one monolayer, which implies the low coverage sticking probability is 0.7 (assuming it is 1 at high coverages). This simple relationship means the dosing time itself can be used to determine coverages, once the time to dose the first monolayer has been determined.

For increasing coverages well beyond a monolayer, the TPD of *n*-hexane resembled that for zeroth-order desorption from a bulk ice: The low temperature peaks for different exposures lined up on the rising edges. For coverages from 4 to 17 monolayers (ML), we fit the leading edge of the TPDs (data not shown here) with an Arrhenius expression for the rate of coverage change $d\theta/dt = \nu \exp(-E_\alpha/RT)$, yielding an

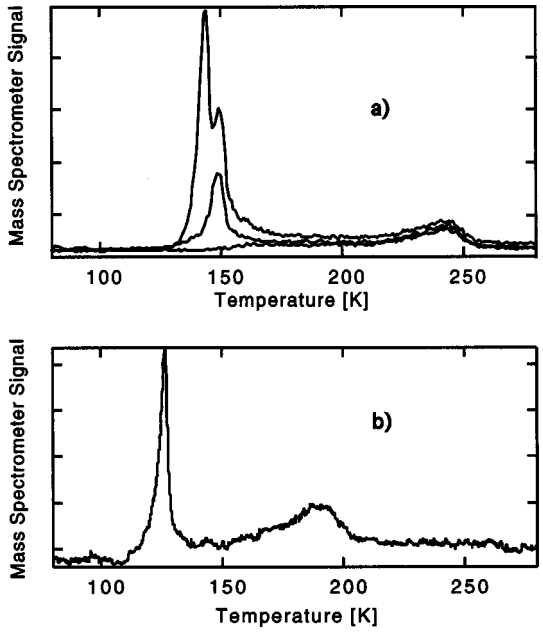

FIG. 3. (a) Temperature programmed desorption spectra shown for 1, 2.1, and 4.5 monolayers of *n*-hexane coverage on Pt(111) (monitoring the $m/q_e=57$ fragment), temperature ramped at 5 K/s. (b) TPD for 3-methylpentane (monitoring mass fragment $m/q_e=41$), 2.5 monolayer coverage, temperature ramped at 0.167 K/s.

E_a of 49 ± 1 kJ/mole, which agrees reasonably well with the enthalpy of sublimation extrapolated from established higher temperature vapor pressures.

Figure 3(b) shows TPD for 3MP. It is similar to that for *n*-hexane, except that first monolayer desorption for 3MP occurred at 190 K and the multilayer desorption for about 2.5 monolayers occurred at 126 K, indicating a lower sublimation energy for 3MP compared to *n*-hexane, as expected.[11] A fit to the leading edge of 45 monolayer desorption data (not shown) to the Arrhenius equation yielded an activation energy of 46 ± 1 kJ/mole.

When the Kelvin probe was used at close proximity to the crystal, each TPD peak was split (see Fig. 5), with the second component appearing at higher temperature and with

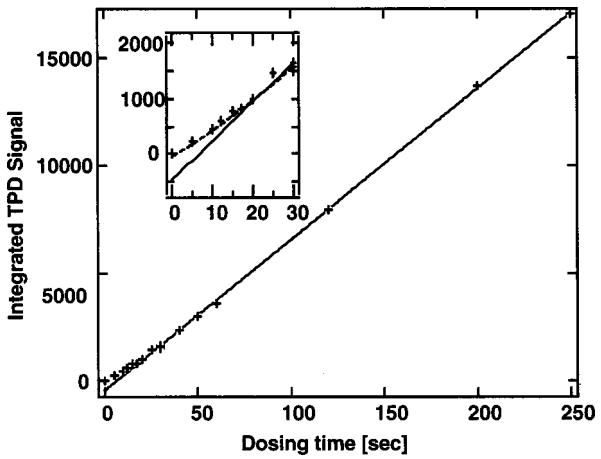

FIG. 4. *n*-hexane sticking probability. Data shown for dosing conditions of 1 cm^3/s (referenced at 1 atmosphere). Deviation from the straight line ceases after the first monolayer is saturated. Inset shows lower exposure times.

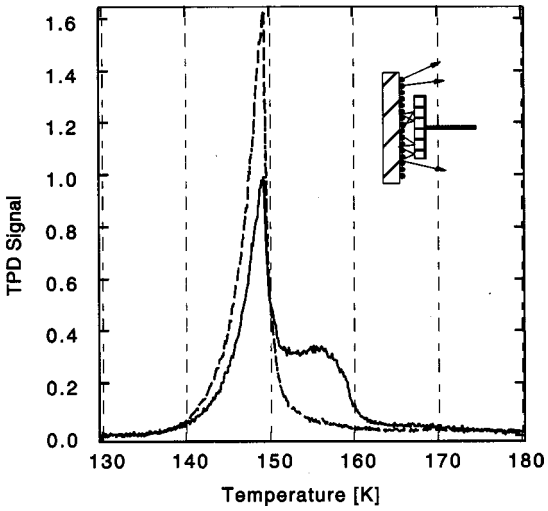

FIG. 5. Kelvin probe blocking effect. TPD signals were modified due to the presence of the Kelvin probe 6 mm disc situated very close to the crystal surface, as indicated by the inset. A 37 monolayer thick film of *n*-hexane was dosed, then desorbed with a temperature ramp of 0.667 K/s. Dashed curve is the signal with no Kelvin probe present and the solid curve is with Kelvin probe present.

larger width. The Kelvin probe tip reflected desorbing molecules back to the Pt crystal, where they readsorbed. This greatly hinders desorption, as is discussed quantitatively in the Appendix.

A gross mass flow rate of 0.8 atm-cm^3/s (corrected for the relative heat capacity of the hydrocarbon vapors, compared to air) through the expansion nozzle was selected for maximum deposition rate and minimum gas load in the ultrahigh vacuum (UHV) chamber, corresponding to a deposition rate of 1/8.0 ML/s for *n*-hexane and 1/7 ML/s for 3MP.

For the conversion of the coverage to *n*-hexane film thickness, the surface density on Pt and in the bulk of the film need to be taken into account. We do know the number of deposited molecules per unit area for our systems. When the material is crystalline, it should be simple to estimate the thickness of the deposit. Extrapolation of density values of both the liquid and the solid phase in the range of 133 to 298 K[12] yielded a density of 0.887 g/cm^3 at 30 K, which corresponds to an average surface density of 3.37×10^{14} molecules/cm^2 (or 29.6 $Å^2$/molecule) and an average spacing between layers of 5.44 Å for crystalline *n*-hexane. This 5.44 Å is (approximately) the spacing we expect for the crystalline hexane. However, we report the dose in terms of ''monolayers,'' based on the coverage to saturate the first adsorbed layer. The number of molecules per square cm in this first monolayer are not expected to have the same value as the number of molecules per square cm in a particular plane of crystalline hexane. We can use the relative packing densities to calculate the film thickness for crystalline hexane of nominally *N* ML thick.

Using the first monolayer density of 2.1×10^{14} molecules/cm^2, a coverage of *N* ML corresponds to a thickness of

$$L=N\times5.44\ \text{Å}\,\frac{2.1\times10^{14}\ \text{molecule/cm}^2}{3.37\times10^{14}\ \text{molecule/cm}^2}$$

$$=N\times3.36\ \text{Å}. \tag{8}$$

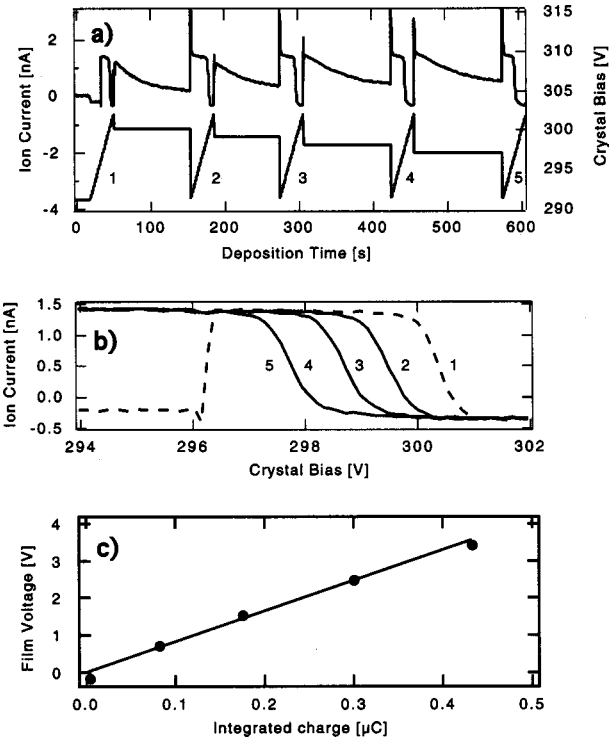

FIG. 6. Cs^+ ion deposition on *n*-hexane thin film at 30 K. (a) Incident ion current (upper trace) as a function of time and independently adjusted crystal bias (lower trace), for 300 eV incident ion beam. Sudden changes in bias caused large displacement currents due to the capacitance of the electrical connections. Sections with constant bias yielded ion accumulation up to the corresponding beam energy. Sections with constant bias slope are used to determine the film voltage [''stopping curves'' shown in panel (b)]. (b) Ion current vs ramped crystal bias. Displacement of the point of steepest descent indicates the film voltage buildup. The early part of trace 1 (between 294 and 296 V), with the ion beam blocked, is below 0 nA because of the current required to charge the electrical cabling as the voltage is ramped. (c) Voltage across the *n*-hexane film due to the accumulation of Cs^+ ions as a function of total delivered ion charge. Film capacitance, given from the graph as the initial inverse slope, was 108 nF, which yields an electric permittivity for *n*-hexane of 1.7.

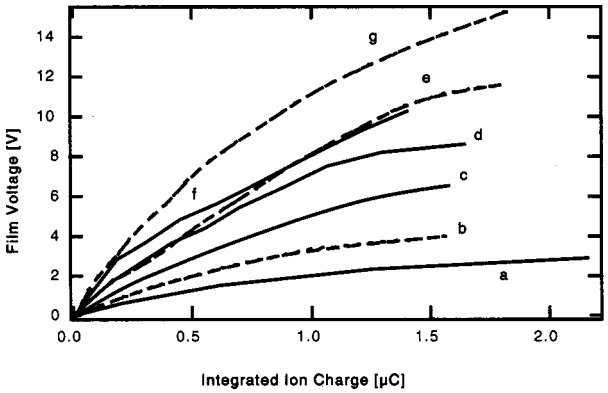

FIG. 7. Film charging at several coverages. Charging curves for amorphous *n*-hexane films of different thicknesses (in ML): (a) 7.5; (b) 12.5; (c) 19; (d) 25; (e) 31; (f) 38; (g) 50.

Vapor-deposited films when amorphous could have considerably less density.[6] But upon heating, they would be expected to compact, probably well before the glass temperature for the strained solid, as it does for amorphous water.[5] This would likely drop the voltage as it will be roughly proportional to the inverse of the square of the density.[5] But, we see no evidence of such a drop, suggesting that unlike water the amorphous hydrocarbons are not particularly ''fluffy'' when deposited at very low temperatures. This is also consistent with our measured capacitances for these amorphous and crystalline hydrocarbon films. So, we assume Eq. (8) holds for amorphous hexane as well. Literature data on 3MP are not as detailed as they are for hexane. As an approximation, we assume that Eq. (8) applies to 3MP, too.

B. Ion current during deposition

The ion deposition stage provided information on the electrical and chemical properties of the adsorbate film. Delivery of 1 eV ions on the molecular film caused charge to build up on the film, thereby preventing further deposition of ions. The effect is illustrated by the decay of the incident ion current as a function of time shown in Fig. 6(a). By reducing the crystal bias, additional ions could be deposited on the film. The voltage buildup could be established from a brief bias ramp while the ion current is monitored. The bias value at which an abrupt current drop appeared indicated how far the film voltage had shifted from the beginning of the ion deposition. A series of such ''stopping curves'' is shown in Fig. 6(b).

The shift of the stopping curves is a direct measure of the charging of the deposited dielectric film. The voltage shifts of the half point of the stopping curves (i.e., the 'film voltages'') have been plotted in Fig. 6(c) versus the ion charge needed to achieve that shift. The charges for each stopping curve are obtained from integration of the ion current with time. A linear dependence of film voltage (V) on film charge (Q), shown in Fig. 6(c) proves that the film is charging up like a capacitor, with the capacitance given by the inverse of the slope of the curve, since capacitance is defined as $C=Q/V$.

The capacitance of a parallel plate capacitor is given by Eq. (1). A was determined from images of the ion beam on a phosphor screen to be 0.4 cm^2. The derivation of the film thickness L was given above. Calculated values for the permittivity based on different samples were close to the literature value for *n*-hexane of 1.9.[11]

The asymptotic value of the ion current rose above 0 for increased values of the film voltage. Part of this nonzero, steady-state current could be attributed to ions impinging upon a bare section of the metal surface (not covered with the insulating molecular film), or, more likely, to gradual local failure of the insulating properties of the *n*-hexane film. Because of these observations, the film capacitance determination was based on the initial slope of the charging curve (Fig. 7).

C. Kelvin probe data: Ions on 3MP

Figure 8 shows the voltage due to D_3O^+ ions deposited on a 45 ML-thick film of 3-methyl-pentane (3MP) as a function of temperature. Up to 70 K the film voltage remained nearly constant, but then dropped at an accelerating rate and reached baseline level by 92 K. According to Eq. (1), a drop

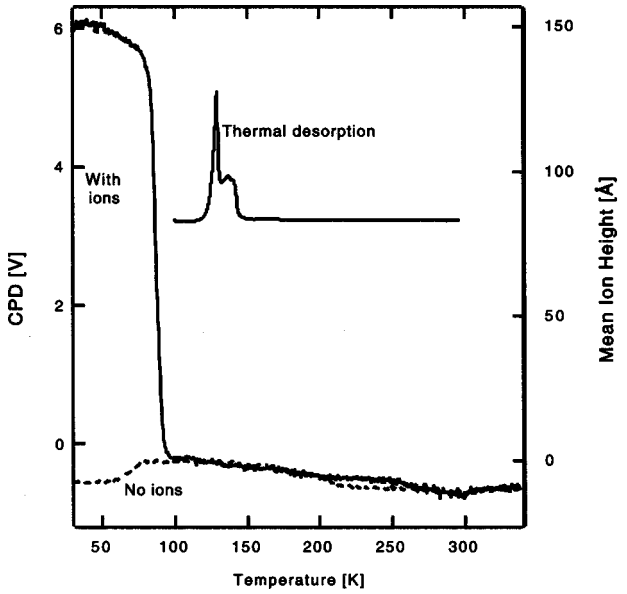

FIG. 8. D_3O^+ ions on a 45 monolayer thick 3MP film at 30 K. With ions, as the temperature was ramped at 0.167 K/s, the generated film voltage dropped near 88 K, where the ion mobility becomes sufficiently high. An approximate distance scale on the right axis gives the average ion location.

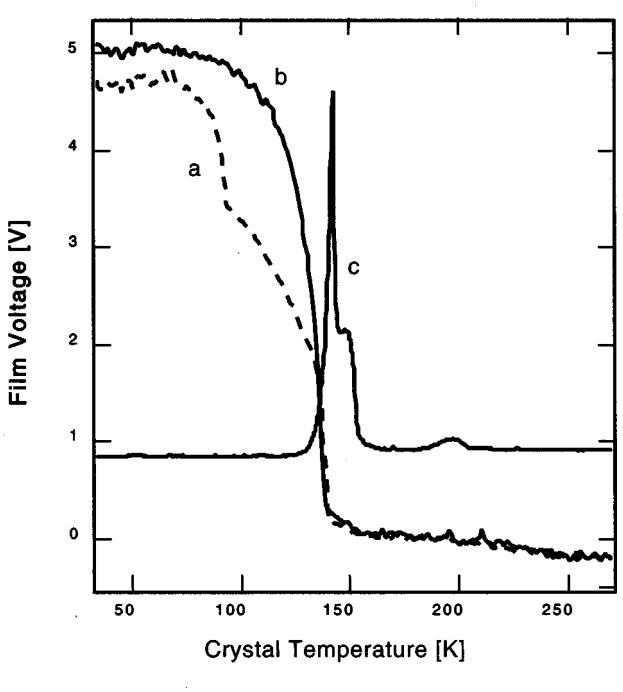

FIG. 9. Voltage on an amorphous 37 monolayer thick *n*-hexane film generated by Cs^+ ions remained nearly constant up to 88 K when it dropped due to thermally activated mobility [trace (a)]. Ion progress was interrupted by the crystallization of the film, which blocked the path of the ions up to much higher temperatures. Baseline level was reached only when the *n*-hexane multilayer film desorbed and the ions nearly reached the Pt substrate. The final voltage drop around 230 K was caused by the change in Pt work function occurring upon desorption of the last monolayer of *n*-hexane. Trace (b) does not show the characteristic voltage drop at 94 K because the film was annealed and hence crystallized prior to the ion deposition, thus preventing any ion motion up to near the desorption temperature. Trace (c) shows the desorbing *n*-hexane. (The small bump near 200 K in curve (c) is not the desorption of the tightly bonded first monolayer, but instead due to stray dosing of slowly heated crystal holder components.)

in the film voltage could be caused by either a loss of charge, an increase in permittivity, or ion migration through the film. Charge loss via electron transfer can be eliminated by several observations: First, electron transfer should depend primarily and very strongly on field strength (as discussed later in more detail), and only weakly on temperature, as kT is very much less than several eV. The voltage drop seen in Fig. 8 is not a strong function of the field, showing a simple ion-mobility proportionality (discussed later). We also have been able to suppress the voltage falloff seen in Fig. 8, by coadsorbing a few monolayers of water with the ions [see related work in Ref. 13). This would not have been expected to be able to strongly influence charge transfer, as the rate-limiting step for this occurs at the lower interface, not the top. Ion size and free-energy effects would be expected to retard ion motion when water is added, as observed. Permittivity of a simple hydrocarbon cannot become much higher than 2, and the voltage change observed would require ε to increase by more than an order of magnitude above 2. Finally, in the similar case of 3MP, as discussed later, the voltage falloff is in reasonable accord with that predicted by ion mobility estimates. These observations leave ion migration as the only reasonable explanation for the major film voltage changes, as seen in Fig. 8.

D. First monolayer work function changes

A final film voltage drop of 0.3 V, which was independent of multilayer coverage or ion dose, occurred at the first monolayer desorption temperature. This is due to the lowering of the Pt work function by 0.3 V by the first monolayer.

E. Ions on hexane

Similar experiments to those done on 3MP, done with *n*-hexane, yielded markedly different results (see Fig. 9). The film voltage, due to either Cs^+ or D_3O^+ (no major differences were observed between Cs^+ and D_3O^+ runs in all of these experiments), dropped in a very similar way up to 90–92 K, but became nearly constant at 95 K at a level higher than 50% of the initial value. The voltage dropped down to baseline at or very near the desorption temperature.

The cause of the difference in behavior between 3MP and *n*-hexane was illuminated by another experiment. Prior to ion deposition, the molecular film of *n*-hexane was annealed up to 120 K for 120 s. As seen in Fig. 9, after the Cs^+ ion dose and during the temperature ramp, the film voltage did not drop appreciably almost until the multilayer desorption. The unannealed *n*-hexane showed intermediate behavior between 3MP and annealed *n*-hexane. Apparently, the annealing process was blocking the movement of the ions whether it happened before the ion deposition (annealed *n*-hexane) or during the temperature ramp (unannealed *n*-hexane). In the latter case, ions could move initially, but were then stopped. Such blocking did not happen in 3MP.

3MP is known not to crystallize under commonly applied procedures, and is often chosen for use because it remains a glass at all temperatures below its melting point.[14] *n*-hexane, which is a linear isomer of 3MP, crystallizes when cooled from the liquid state. Vapor-deposited *n*-hexane is

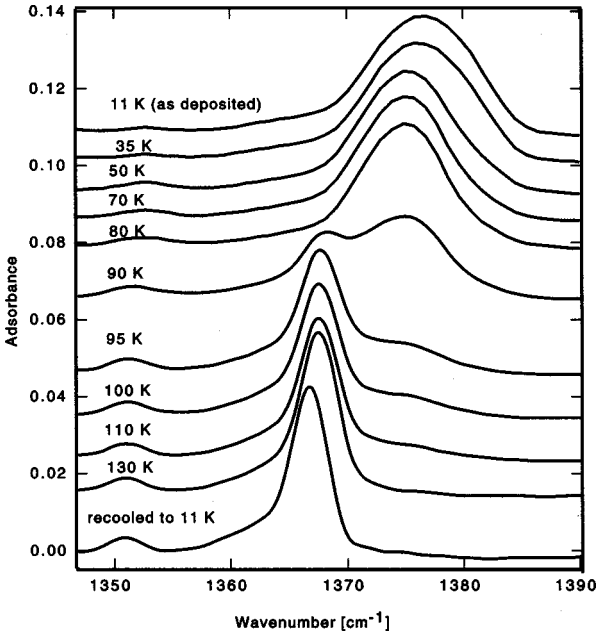

FIG. 10. A series of FTIR spectra recorded during heating of a 1 micron thick *n*-hexane film, at about 0.17 K/s. A distinct irreversible structural change occurred between 80 and 95 K, which corresponds to the crystallization of the material.

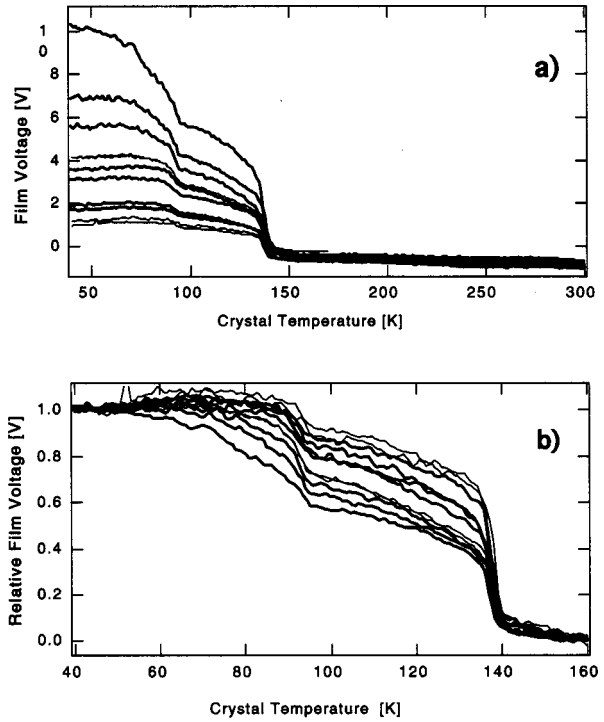

FIG. 11. Field-dependent motion of ions in unannealed *n*-hexane. (a) Different initial film voltages across same thickness amorphous films (37 ML) exhibit the same qualitative features as the temperature is ramped at 0.167 K/s, but the detailed curve shapes depend on the electric field intensity. (b) The effect becomes clearer when the measurements in (a) have been scaled to their starting values. The curve with the largest relative drop (bottom curve) corresponds to the highest initial voltage [top curve in (a)].

amorphous and crystallizes when the temperature is high enough to overcome the activation energy barrier.

F. FTIR of *n*-hexane

The change of *n*-hexane structure was confirmed through Fourier-transform infrared (FTIR) spectroscopy. A 1 μm thick film of *n*-hexane was deposited on KBr at 11 K. Several spectra were recorded between 11 and 130 K as the temperature was ramped. Figure 10 shows the changes in peak positions and shapes for CH_2 and CH bends occurring in the 1350–1390 cm^{-1} range. Spectra taken below 90 K are very similar to each other, and so are those taken above 90 K. Upon heating, the features of the spectrum shifted in frequency and became narrower, indicating a change to a more ordered, crystalline-like structure. This narrowing was seen in all the vibrational bands of *n*-hexane, not just the ones shown. At 90 K, where the system seems to be partly crystallized, one might imagine crystalline regions imbedded in an amorphous ''melt.'' Upon cooling back down to 11 K, the original spectrum was not recovered, indicating an irreversible structural change. Furthermore, since the FTIR measurements did not involve any ions, we conclude that the crystallization observed through film voltage measurements was not caused by the presence of the ions. Also note the slight narrowing of the peak between 11 and 50 K, suggesting that the amorphous *n*-hexane is structurally metastable as deposited at very low temperatures, similar to amorphous water.[5]

G. Field dependence of ion motion

If the ions move with a classic ion mobility, this should be clearly evident from a study of the ion motion as a function of electric field. For simplicity, this study would have best been done for the 3MP case, but for various reasons, it was done for the *n*-hexane case. Here, we should expect that the ions would find, as the temperature is ramped, that the amount of amorphous liquid through which they could move was a strong decreasing function of T, reaching nearly zero at 95 K. Also, the ions feel a broad range of field strengths, from a maximum given by $1/L$ times, the voltage from Eq. (3), to a minimum of zero. While this is a complicated situation, if the ions have a velocity proportional to the field strength, then, to first order, the average distance the ions move during the time of the ramp from low temperature through, say 95 K, will be proportional to the field strength. Figure 11 shows data for a constant film thickness, as the amount of ions is varied. The data are shown both as originally taken and as rescaled to their initial voltage. The rescaled data emphasize the ion-motion aspect, as the curves are directly proportional to the mean ion height [Eq. (4)]. The systematic changes in ion motion versus field are evident, and will be discussed later.

Annealed films, presumably all crystalline, were studied under several different conditions. The behaviors were all very similar to that seen in Fig. 9; that is, very limited or no ion motion until near the desorption temperature. No dependence on field intensity was apparent. One curious feature did stand out, however, as shown in Fig. 12. The voltage drop occurred just before the *n*-hexane desorbed about half the time, while at other times, under nominally the same conditions, it would occur during the *n*-hexane desorption. This will be discussed later.

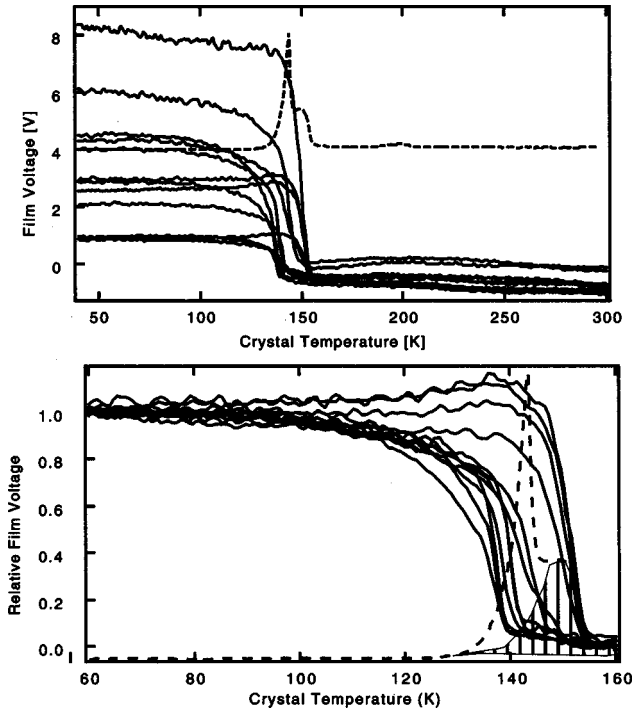

FIG. 12. Scatter in steep drop, annealed *n*-hexane. Film voltage vs temperature for annealed, same thickness *n*-hexane films (37 ML). No systematic dependence in steep drop behavior on initial voltage is observed. Dashed curve is typical temperature programmed desorption signal for *n*-hexane. In the lower panel, the curves are scaled to their low-temperature initial voltage. Shaded region is approximately the desorption signal coming from behind the Kelvin probe. The ramp rate used was 0.33 K/s. Annealing prior to Cs^+ deposition was performed at 120 K for 120 s.

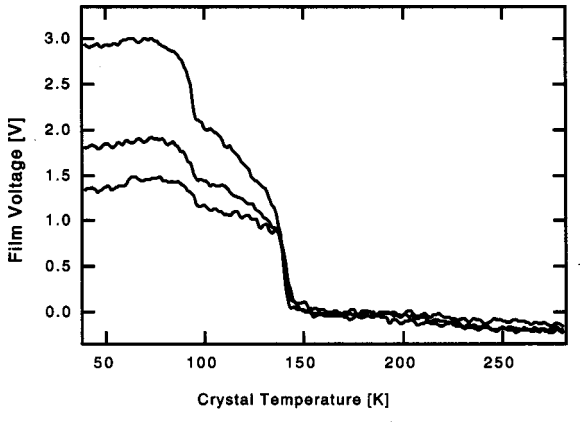

FIG. 13. Electron effects. Film voltage profiles on amorphous *n*-hexane after deposition of similar amounts of Cs^+ ions on same thickness films (37 ML). Films differ by the number of 300 eV electrons intentionally deposited on the film after the Cs^+ deposition. From top to bottom, the amount of electrons deposited was 0, 0.13, and 0.20 μC. The magnitude of the voltage changed, but not the shape of the curve.

H. Effect of electrons

A small number of electrons were found to exist in the ion beam because of collisions of the ions with a thin mesh close to the crystal target. They were present at about 2% of the ion beam flux when the ions passed through the ion decelerator meshes. However, when the target bias was adjusted to repel most of the ions, the ions hit the deceleration meshes from the target side and the electron current rose several-fold, sometimes to as high as 20% of the incident ion flux. These secondary electrons, likely formed with only a few eV of energy at the mesh, were then accelerated to around 300 eV by the time they hit the sample. This required careful consideration, as electrons of this energy could severely damage the hydrocarbon film[15] (since these data were taken, these electrons have been eliminated by means of a magnetic field). One major saving feature is that, typically on order of 0.1% of a monolayer of ions was deposited, so lesser numbers of electrons may do negligible damage. Their actual effect was studied by purposely dosing electrons on unannealed *n*-hexane thin films after depositing Cs^+ ions, at fluences both equal to, and considerably exceeding, our typical estimated dose during ion deposition. As seen in Fig. 13, it was found that a prolonged 300 eV electron dose reduced the measured film voltage without significantly changing its dependence on temperature. Although associated TPD data indicate a small drop in the amount of desorbing *n*-hexane, which was almost within our error bars, an increase in carbon contamination of the Pt surface after the desorption suggested partial decomposition of *n*-hexane.

The possibly detrimental results of electron impact on the hexane films, such as electron-induced dissociation, have been studied by other researchers.[15] This could have only limited effects on our experiments: Assuming a dissociation cross section of 18 Å^2,[16] a total ion charge delivered to the film of order 1 μC, and a typical electron dose at least an order of magnitude less, no more than a fraction of 0.1% of hexane would react. Thus, our measurements were not affected in any quantitative way under our standard operating conditions, as far as the molecular film was concerned. Electron flux emitted from the mass spectrometer ionization filament was even lower and could only contribute during part of the TPD.

I. Maximum film voltage

During ion deposition, it was found that the capacitor model for the thin film would hold for a range of voltages, but after a certain value the film voltage could not be increased further. The effect was not studied in detail. However, for several films, it was found that typically the voltage would simply cease increasing with additional ion charge deposited. If the ion current was halted and the film voltage checked after various delays (via the stopping curve for the ion beam), typically we found that the film voltage did not decrease with time. The implication is that the maximum voltage reached is not, for example, a simple equilibrium between an incident ion current and a resistive leakage through the film. The curves of Fig. 7 were extrapolated to estimate the maximum voltage obtainable. This is most accurate at 7.5 and 37 monolayer coverages (the former was nearly saturated, and for the latter we have other data to confirm the extrapolation). Maximum obtainable voltages are shown in Fig. 14.

Similar experiments were done for ion motions on hexane using D_3O^+ instead of Cs^+. These figures are not pre-

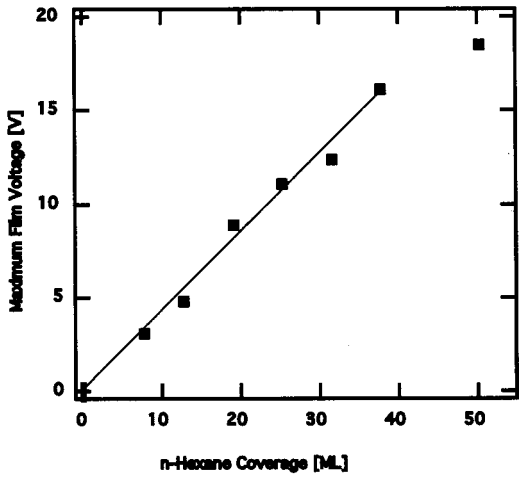

FIG. 14. Maximum voltage attainable vs coverage. Extrapolation of the curves shown in Fig. 7 using exponential yielded the estimated maximum voltage across *n*-hexane films of different thicknesses. The maximum field intensity sustained given by the slope was 0.43 V/ML or 1.3×10^9 Vm^{-1}.

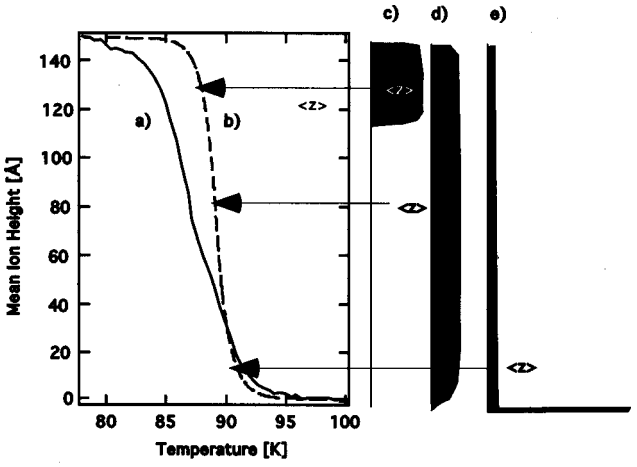

FIG. 15. Predicted ion motion. Curve (a) is the experimental data from Fig. 8, expanded near where the ions move. Curve (b) is that predicted by the Stokes–Einstein relation between ion mobility and solvent viscosity. Diagrams on the right illustrate charge distributions, specifically (c) shortly after they begin significant motion, (d) just as the leading edge hits bottom, and (e) as charge piles up at $z=0$, respectively.

sented here. But in general, the results were very similar to those seen when Cs^+ was used. As the ion sizes that should determine the ion mobilities should be similar for both these ions, this similarity is not unexpected.

IV. DISCUSSION

A. Comparison with 3MP viscosity data

The motions of ions within a liquid, including glasses above their glass-transition temperature, are mostly a function of the viscosity of the material. The well-known Stokes–Einstein equation for the mobility of an ion of charge nq_e is based on the formula for the viscous drag on a macroscopic sphere of radius r moving in a fluid of viscosity η, and is

$$\mu(T)=\frac{nq_e}{6\pi r\,\eta(T)}. \tag{9}$$

The viscosity of 3MP has been reported in several papers,[17] even down to 77 K,[14] as it is a prototypical glass-forming material. Integration of the field-induced motion effects on the initial near delta-function spatial distribution of ions can be done nearly in closed form. Any initially narrow distribution can be easily shown to quickly become a square distribution. The temporal dependence of the corresponding voltage changes form when the leading edge of the distribution reaches the bottom of the film, i.e., when $V_{\text{film}}=V_0/2$, as illustrated in Fig. 15, diagrams (c), (d), and (e). The voltage versus time thus has different functional forms before and after this moment

$$V_{\text{film}}(t)=V_0\cdot\left[L-t\frac{V_0}{2L}\overline{\mu}(t)\right]\cdot\frac{1}{L}\quad\text{for } V_{\text{film}}\geqslant\frac{V_0}{2}, \tag{10a}$$

$$V_{\text{film}}(t)=\frac{L^2}{2t\overline{\mu}(t)}\quad\text{for } V_{\text{film}}<\frac{V_0}{2}, \tag{10b}$$

$$\text{with } \overline{\mu}(t)\equiv\frac{1}{t}\int_0^t dt'\cdot\mu(T(t'))$$

$$\approx\frac{nq_e}{6\pi r}\frac{1}{t}\int_0^t dt'\cdot\frac{1}{\eta(T(t))}, \tag{10c}$$

where V_0 is the initial film voltage when the ions are all at the top of the film, and the Stokes–Einstein approximation is used in (10c). The time integral works for any temperature versus time function, not just a linear ramp. Equation (10b) interestingly does not depend on V_0, and it depends on L only via a simple L^2 factor. This means that the time-dependent film voltages for two differing initial values of charge and L will superimpose if rescaled by $1/L^2$, over that temperature range where both curves are less than half their initial voltage. We numerically integrate $1/[\eta(T(t))]$, using Arrhenius-like expressions fit to published measurements for $\eta(T)$.

Ling and Willard[14] give $\log(\eta(T))=3460/T-32.2$ for $77.5\,\text{K}<T<94.5\,\text{K}$. If we arbitrarily set r_{ion} to 3 Å, we calculate the curve (b) in Fig. 15. The results are a fairly close match to the experimental results [Fig. 15, curve (a)], but our predicted voltage falloff is displaced about 3 K to higher temperature. A better match could be had using an order of magnitude smaller r_{ion}, but this is not physically meaningful. It may be due in part to a possible ±2 K error for our measurement of the sample temperature. Also note that the experimental voltage falls over a two to three times wider temperature range than that of the predicted curve. We have not attempted to resolve the reason for this extra width experimentally, but we introduce some hypotheses, some of which are easily testable: (1) The mobility may not follow the Stokes–Einstein model; (2) the film varies somewhat in thickness, with the thinner areas having higher fields and shorter distance to move, so they would contribute to a net lowering and broadening of the curve; (3) surface diffusion of the ions (or solvent molecules) either permits ions to seek

out low places, or solvent molecules to climb on top of the ions; (4) amorphous materials are inherently patchy in structure, and 37 monolayers is not thick enough to average out the properties; (5) the viscosity and mobility differ near the solid interface from their bulk values; and (6) the fields are high enough to prevent a linear mobility from being valid.

B. Mobility in hexane

1. Field dependence

The field dependence of the motion can be examined, using the data for *n*-hexane, from Fig. 11. Admittedly, it would be easier to interpret if similar data had been taken for 3MP, which unlike *n*-hexane shows no sign of crystallization. A qualitative analysis can be made of the ion motion: Before crystallization, the various curves of Fig. 11(b) fan out, the highest field curves showing the largest relative motion. After freezing is complete (95 K), the data still show some slow ion motion, but the curves all move more or less in parallel. Thus, the ion motion in liquid *n*-hexane is roughly proportional to the field strength. But after freezing, its motion is independent of field strength. Perhaps in the latter case, ions move only as polycrystalline grain boundaries move.

We attempt a more quantitative assessment. While *n*-hexane is crystallizing, the ions will have to move in progressively smaller channels. Referring back to Eq. (10), for a homogeneous medium, the distance the ion moves involves an integral over the ''fluidity'' $(1/\eta(T(t)))$ of the medium. Without attempting to mathematically justify it, it is still not unreasonable to suspect that as long as the medium crystallizes independently of the field (this is a nonpolar molecule), the net motion at any time ought to be roughly proportional to the field strength times the opportunity for motion [the latter being some time integral of (effective liquid channel fraction)$/\eta(T(t))$]. All the data of Fig. 11 show a strong bend at the same temperature, 95 K, suggesting that the crystallization is indeed independent of the field strength. Since the bends all occur before the average ion reaches halfway through the film, and thus the fastest ion should not yet have reached the film bottom, we are in the limit of Eq. (10a). Then, we expect to find a linear dependence of the total motion by 95 K on the field strength, if a linear ion mobility is operative. Figure 16 shows the fractional voltage drop as a function of field intensity. Also shown is a line going through the origin that roughly fits the data. There appears to be modest curvature, and a quadratic fit (also constrained to go through zero) does fit better. While some indication is seen that a linear mobility may not be valid at 5×10^8 V/m, the fact that at lower fields the curve is fairly linear, and extrapolates roughly back to the origin, supports field-driven motion.

2. Motion required for crystallizing hexane

We can get a measure of how much molecular motion is required to crystallize *n*-hexane, in a curious way. The ion motion before freezing, shown in Fig. 16, might just as well be applied to a neutral molecule. That is, if we use the Einstein relation from Eq. (5) at any temperature, a neutral molecule will move with a D given by $kT/\eta(T)$ times the mobility. Over the range of temperatures where the ions are moving, the temperature is essentially constant. From Eq. (10), the amount the ions move is proportional to the time integral of $\eta(t)$. Thus, the amount the ions move before crystallization should be proportional to the time integral of D. From the slope in Fig. 16 of 24 Å/(10^8 V/m), we get Eq. (11):

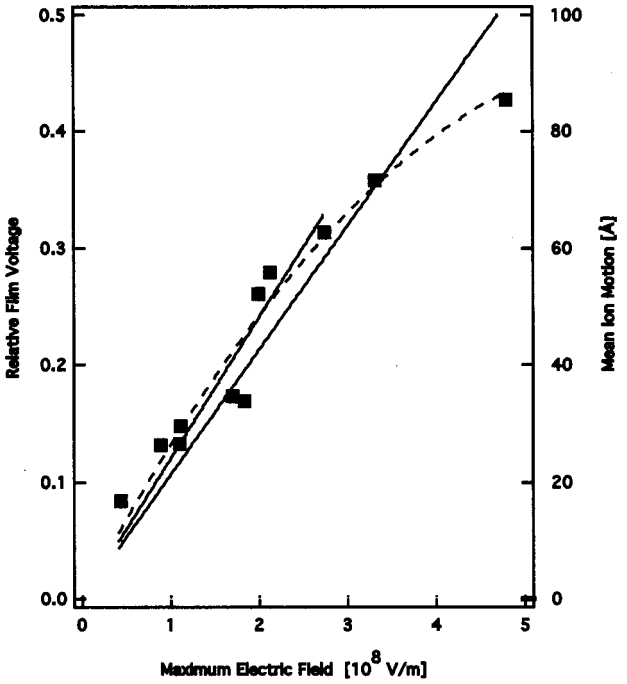

FIG. 16. The relative voltage drop reached by 95 K in Fig. 11 are displayed vs electric field intensity for each sample. Two lines (passing through zero) shown are fits to either all the data, or excluding the two highest field points. A quadratic fit to all the points passing through the origin is also shown (dashed curve).

$$2.4\times10^{-17}\,\mathrm{m^2/V}=\left[\frac{t\overline{\mu}(t)}{2}\right]=\frac{1}{2}\int_0^t dt'\cdot\mu(T(t'))\approx\frac{nq_e}{2kT}\int_0^t dt'\cdot D(T(t')). \tag{11}$$

This gives the time integral till total freezing of D of $3.9\times10^{-19}\,\mathrm{m^2}$. Now, in the context of a random walk, D is also equal to the hop distance squared times the rate of hopping. Thus, a time integral of D should be equal to the hop distance squared times the number of hops. The mean excursion distance is just the square root of this. Thus, a Cs^+ ion in *n*-hexane, under field-free conditions, should have hopped a total distance of 6 Å. To the extent our Stokes–Einstein relation works, with $r_{\mathrm{ion}}=3$ Å, which is also about half of an *n*-hexane molecule size, our data suggest that *n*-hexane freezes when the *n*-hexane molecules diffuse a net distance of about 1 molecule.

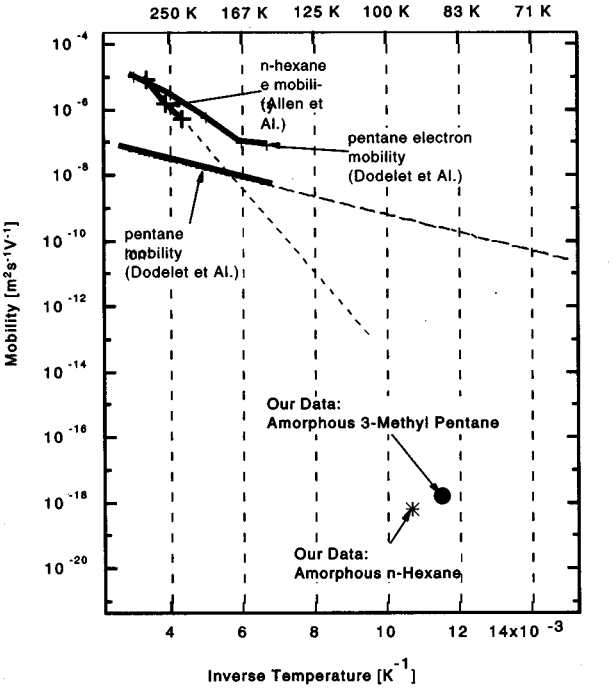

FIG. 17. Mobilities vs temperature. Along with our data, shown are electron mobilities in *n*-hexane (Ref. 21) and pentane (Ref. 18), and pentane ion mobility in pentane (Ref. 18). Broken lines are added to indicate the trends implied by the available data. Our data cover a very different temperature range.

3. Possible grain boundary effects

An interesting fact mentioned earlier was that for preannealed, crystallized *n*-hexane, about half of the time the voltage drops to nearly zero around 140 K, just before the *n*-hexane desorbs, and the other half during *n*-hexane desorption near 155 K, as seen in Fig. 12. Occasionally, the voltage drops as if a hybrid of the two. Referring to Fig. 9, this kind of behavior is not seen for putting ions on top of amorphous *n*-hexane and heating, which creates crystallized hexane near 95 K. In Fig. 9, we see that the final voltage drop always occurs near 140 K, at the start of the *n*-hexane desorption. We offer the suggestion that any ion motion in crystallized hexane occurs only along grain boundaries. Sometimes, when a sample is crystallized by preannealing, as in Fig. 12, there are no grain boundaries at all, so ion motion occurs only due to actual film loss.

C. Comparison to other measurements of mobility

While some viscosity information exists for good glass formers like 3MP (but not *n*-hexane, as it is not a stable glass former under more usual methods), permitting one to estimate ion mobility, there are very few direct measurements of ion mobilities in organic glasses. Even when viscosities are known, the mobility can be proportional to powers of the viscosity from -1 to -1.3.[18] Direct studies of ion mobility typically suffer from lack of knowledge of the actual ion identity, unknown effects of counterions, and poor geometrical information. Figure 17 puts our data onto a graph containing some related literature data that measure ion mobility at other than just room temperature. We also include some electron mobility data (typically several orders of magnitude faster than ions). Because of our extraneous temperature width for our data, we do not claim any real knowledge of the temperature dependence of the mobility. What the plot indicates is how many orders of magnitude away other measurements are from ours, mostly because we are studying this material when it is so extremely viscous.

D. Maximum voltage reached

Here, we discuss the maximum voltages that we could apply to the films. The films act as if they have a sudden-onset breakdown voltage, or in some cases, a distribution of sudden-onset breakdown voltages. From Fig. 14, we see the maximum voltage reached is reasonably linear in film thickness, suggesting that the maximum electric field that the films can hold off is a constant independent of coverage. From Fig. 14, this is 1.3×10^9 V/m. One obvious possibility is that we are seeing electron emission into the films, due to the high field strength. As per the famous Fowler–Nordheim formula, the current expected to tunnel out of a metal over a triangular barrier of height w, with field strength E is[19]

$$I = 1.54\times10^{10}\frac{E^2}{w}(\mathrm{Am}^{-2}(\mathrm{m/V})^2(\mathrm{eV})) \times e^{-(6.8\times10^9\ \mathrm{Vm}^{-1}/E(w/\mathrm{eV})^{3/2})}. \quad (12)$$

The barrier height should be something like the bare Pt work function voltage, 5.7 eV, plus the stabilization V_0 that the electron feels in amorphous *n*-hexane compared to being in a vacuum. The latter is not known for vapor deposited *n*-hexane at 30 K, but using the value of V_0, $+0.21$, for liquid *n*-hexane at 193 K (measured by photoelectron threshold measurements from zinc electrodes into solvent versus into vacuum[20]), and extrapolating it with the measured T-slope of -0.0024 eV/K to 30 K gives V_0 of 0.6 eV. This gives $w\approx6.3$ eV. Using Eq. (12), the calculated currents versus field and barrier height are shown in Fig. 18. Using the maximum voltage obtainable from Fig. 14, the maximum field strengths are about 1.3×10^9 V/m. In Fig. 18, we see that at $w=6.3$ eV and at 1.3×10^9 V/m, the expected electron current would be orders of magnitude smaller than the 10^{-5} Am^{-2} needed to stop charging due to the incident ion beam. However, at about three times this field, there would be enough field-induced electron emission to stop the charging. One possibility is that the film has thin spots of perhaps one-third the mean thickness, and thus three times the field strength. There, electrons could be amply transmitted. Once the electrons tunnel through the weak spot, they probably would have ample mobility to move laterally, to spread current over considerable areas. High electron mobility is, of course, suggested by the data in Fig. 17.

Another possibility is that the ions themselves are moving. We have evidence in further work[13] that ion motion in methyl cyclohexane can be induced at progressively lower temperatures as the field is increased over 10^8 V/m, even well below the glass temperature. This ion motion is perhaps akin to dielectric breakdown processes (partially) understood to occur in the field regime of 10^9 V/m.[19] At this point, we are not sure whether ion or electron motion stops the charg-

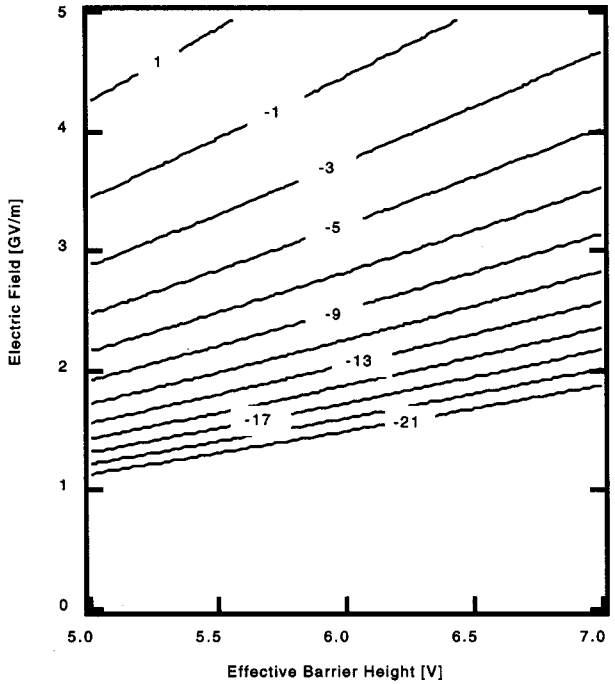

FIG. 18. Shown is the plot vs barrier height and field strength of the electron emission predicted by the Fowler–Nordheim formula [Eq. (12)]. The contours show the log of the current in A/m^2. Approximately 10^{-5} A/m^2 is needed to stop the films from charging.

ing. Some obvious ways to find out would include changing the work function of the substrate, or putting blocking layers at the film bottom, to stop the electrons, or near the top, to stop the ions.

V. CONCLUSIONS

This paper reports on innovative approaches to measuring motions of ions in hydrocarbons. Both Cs^+ or D_3O^+ behave similarly. Ion motion in 3MP was particularly simple, and occurred at the temperature predicted by simple viscosity-based estimates of ion mobility. However, the range of temperatures during the temperature ramp over which the ions moved was two to three times that predicted by the theory, suggesting that the 3MP film has some inherent microheterogeneity. Hexane was similar to 3MP, except for the interruption of the ion diffusion by crystallization of the hexane near 95 K. We estimate that the neutral hexane molecules need only move about 1 molecular diameter for crystallization to occur. We see some differences in higher temperature (140–160 K) ion motion in hexane, depending on whether it crystallized with the ions in place, or was precrystallized. This dependence supports our notion that ion motion occurs along grain boundaries in polycrystalline hexane. The maximum field strength that hexane could maintain was 1.3×10^9 V/m. This is a factor of 3 lower than the limit expected for field emission of electrons to halt charging. Nonviscosity mediated motion of the ions themselves may limit the maximum voltage. In general, the simplicity and directness of the soft-landing ion approach suggest that it should be applicable to a wide range of problems.

APPENDIX: KELVIN PROBE EFFECT ON TPD PEAK SHAPE

The Kelvin probe causes the TPD peaks to be distorted, as mentioned earlier. Here, we discuss the effect more quantitatively. The process for molecules getting out from behind the Kelvin probe is basically a random walk, with parameters as follows: The Kelvin probe is a 6 mm ($=S$) disc, which during operation is about 0.1 to 1 mm away ($=B$) from the target, as shown in Fig. 5. A molecule on the sample that desorbs from the region behind the Kelvin probe will most likely hit the Kelvin probe, except for those that leave the outermost annular region of width about B (these latter molecules have about a 50% chance of missing the opposing Kelvin probe). Those that hit the Kelvin probe will not linger on it for long, since they will typically have a much shorter residence time on gold near room temperature than they do on the cold sample. So, they will desorb after an insignificant residence time, and typically hit the sample roughly within a distance B of where they started.

Now, assuming that the molecules desorb with a $\cos(\theta)$ distribution, where θ is the angle from the surface normal, the most likely exit angle is ±45 deg from the normal. Properly averaging over all azimuths and polar angles, a molecule will on the average change its radial position by $B/2$ for each hop across the gap. So, getting out away from the sample is really a random walk on the radius, with $B/2$ being the step size. We have numerically modeled this random walk desorption process, and the predicted waveform agrees well with that seen in the figures, such as Fig. 5. But a simpler analysis can estimate the effect in a closed analytical form. Each desorption step (i.e., random walk step) takes a time equal to half the surface lifetime on Pt, since half the hops—the ones on Au—do not have substantial lifetimes. Unlike the time it takes for a molecule to desorb, the number of hops it takes to escape radially is determined geometrically, independent of the desorption kinetics. If we assume the typical molecule starting out under the Kelvin probe lies $S/4$ from the edge, then the random walk must move $(S/4)/(B/2)$ net steps to escape, or $S/2B$. For B between 0.1 and 1 mm and $S=6$ mm, this number varies from 30 to 3 net steps. A random walk will require the square of the ratio of the net motion to the step size to achieve this on the average. Thus, 900 to 9 hops will be needed to escape over a period of 450 to 4.5 surface lifetimes. The effect on the desorption kinetics is essentially like decreasing the desorption pre-exponential by a factor of 1/450 to 1/4.5. From Ref. 16, the peak temperature of desorption T_p for a multilayer deposit with simple zeroth-order Arrhenius desorption with a linear temperature ramp should be about

$$T_p=\frac{E_a}{R}\left(\ln\left[\frac{0.94\nu/NE_a}{(\theta_0-1)\sigma_{\mathrm{ML}}\beta R}\left(\frac{RT_p}{E_a}\right)^2\right]\right)^{-1}$$

$$\approx\frac{E_a}{R}(30-\ln(N))^{-1}, \tag{13}$$

where θ_0 is the initial coverage, E_a is the Arrhenius activation energy, ν is the pre-exponential, β is the heating rate, R is the gas constant, and σ_{ML} is the surface density of the adsorbate. In the above, we insert N, the surface lifetimes

spent in escaping from behind the Kelvin probe, with $N = S/4B$. If $T_p = 149\,\mathrm{K}$ with $N = 1$, then the effect of the blocking should force T_p to become about 187 to 157 K for $L = 0.1$ to 1 mm. Figure 5 shows TPD for a 37 monolayer *n*-hexane film, with and without the Kelvin probe in front of the sample. With the Kelvin probe, about 36% of the desorption should occur from behind it, 64% from around it. As the broad peak has a maximum at about 158 K, this is compatible with a Kelvin probe spacing of about 1 mm.

ACKNOWLEDGMENTS

Supported by Offices of Chemical Sciences of the Basic Energy Sciences Division of the Department of Energy. The Environmental Molecular Sciences Laboratory is supported by the DOE Office of Biological and Environmental Research. Pacific Northwest National Laboratory is a multiprogram national laboratory operated by Battelle Memorial Institute for the Department of Energy. We thank J. Bradley Rowland and Wayne P. Hess for recording the FTIR spectra of *n*-hexane.

[1] J. P. Cowin, A. A. Tsekouras, M. J. Iedema, K. Wu, and G. B. Ellison, Nature (London) **174**, 398 (1999); J. P. Biesecker, G. B. Ellison, H. Wang, M. J. Iedema, A. A. Tsekouras, and J. P. Cowin, Rev. Sci. Instrum. **69**, 485 (1998).

[2] In many cases, to prevent too much motion during setup of an experiment, preparation can be done below the glass temperature.

[3] F. D. Wagner, ''Simulation of the Electrochemical Double Layer in Ultrahigh Vacuum,'' in *Structure of Electrified Interfaces*, edited by J. Lipkowski and P. N. Ross (Wiley-VCR, New York, 1993), pp. 309–400.

[4] A. W. Kleyn, Science **275**, 1440 (1997); S. A. Miller, H. Luo, S. J. Pachuta, and R. G. Cooks, *ibid.* **275**, 1447 (1997).

[5] A. A. Tsekouras, M. J. Iedema, and J. P. Cowin, Phys. Rev. Lett. **80**, 5798 (1998).

[6] D. E. Brown, S. M. George, C. Huang, E. K. L. Wong, K. B. Rider, R. S. Smith, and B. D. Kay, J. Phys. Chem. **100**, 4988 (1996).

[7] P. W. Atkins, *Physical Chemistry*, 3rd ed. (Freeman, New York, 1986), Chap. 27.

[8] J. L. Brand, M. V. Arena, A. A. Deckert, and S. M. George, J. Chem. Phys. **92**, 5136 (1990).

[9] A. R. Bishop, M. J. Hostetler, G. S. Girolami, and R. G. Nuzzo, J. Am. Chem. Soc. **120**, 3305 (1998).

[10] L. E. Firment and G. A. Somorjai, J. Chem. Phys. **66**, 2901 (1977).

[11] *CRC Handbook of Chemistry and Physics*, edited by D. R. Lide, Ed. 78th ed. (CRC Press, Boca Raton, 1997).

[12] *Thermodynamic Tables-Hydrocarbons* (Thermodynamics Research Center, College Station, TX, 1992), pp. d-101–1011.

[13] K. Wu, M. J. Iedema, and J. P. Cowin, Langmuir (submitted).

[14] A. C. Ling and J. E. Willard, J. Phys. Chem. **72**, 1918 (1968).

[15] T. Mastushige and W. H. Hamill, J. Phys. Chem. **76**, 1255 (1972).

[16] C. Xu, and B. E. Koel, Surf. Sci. Lett. **292**, L803 (1993).

[17] G. Fischer and E. Fischer, Molec. Photochem. **8**, 279 (1977).

[18] J.-P. Dodelet, G. R. Freeman, Can. J. Chem. **55**, 2264 (1977).

[19] R. Coelho, *Physics of Dielectrics for the Engineer* (Elsevier Scientific, NY, 1979), p. 124.

[20] R. A. Hoylroyd, S. Tames, and A. Kennedy, J. Phys. Chem. **79**, 2857 (1975).

[21] A. O. Allen and R. A. Holroyd, J. Phys. Chem. **78**, 796 (1974).